Ageeva, A.; Khramtsova, E.; Magin, I.; Purtov, P.; Miranda Alonso, MÁ.; Leshina, T. (2018). Role of association in chiral catalysis: from asymmetric synthesis to spin selectivity. Chemistry - A European Journal. 24(70):18587-18600. https://doi.org/10.1002/chem.201801625

CHEMISTRY
A European Journal

A Journal of
ChemPubSoc Europe

Accepted Article

Title: Role of association in chiral catalysis: from asymmetric synthesis to spin selectivity

Authors: Aleksandra Andreevna Ageeva, Ekaterina A. Khramtsova, Ilya M. Magin, Peter A. Purtov, Miguel A. Miranda, and Tatyana V. Leshina

To be cited as: *Chem. Eur. J.* 10.1002/chem.201801625

Link to VoR: http://dx.doi.org/10.1002/chem.201801625

Supported by
ACES

WILEY-VCH

10.1002/chem.201801625

WILEY-VCH

Role of association in chiral catalysis: from asymmetric synthesis to spin selectivity

Aleksandra A. Ageeva,*[a] Ekaterina A. Khramtsova,[a,b] Ilya M. Magin,[a] Peter A. Purtov,[a,b] Miguel A. Miranda,[c] Tatyana V. Leshina[a]

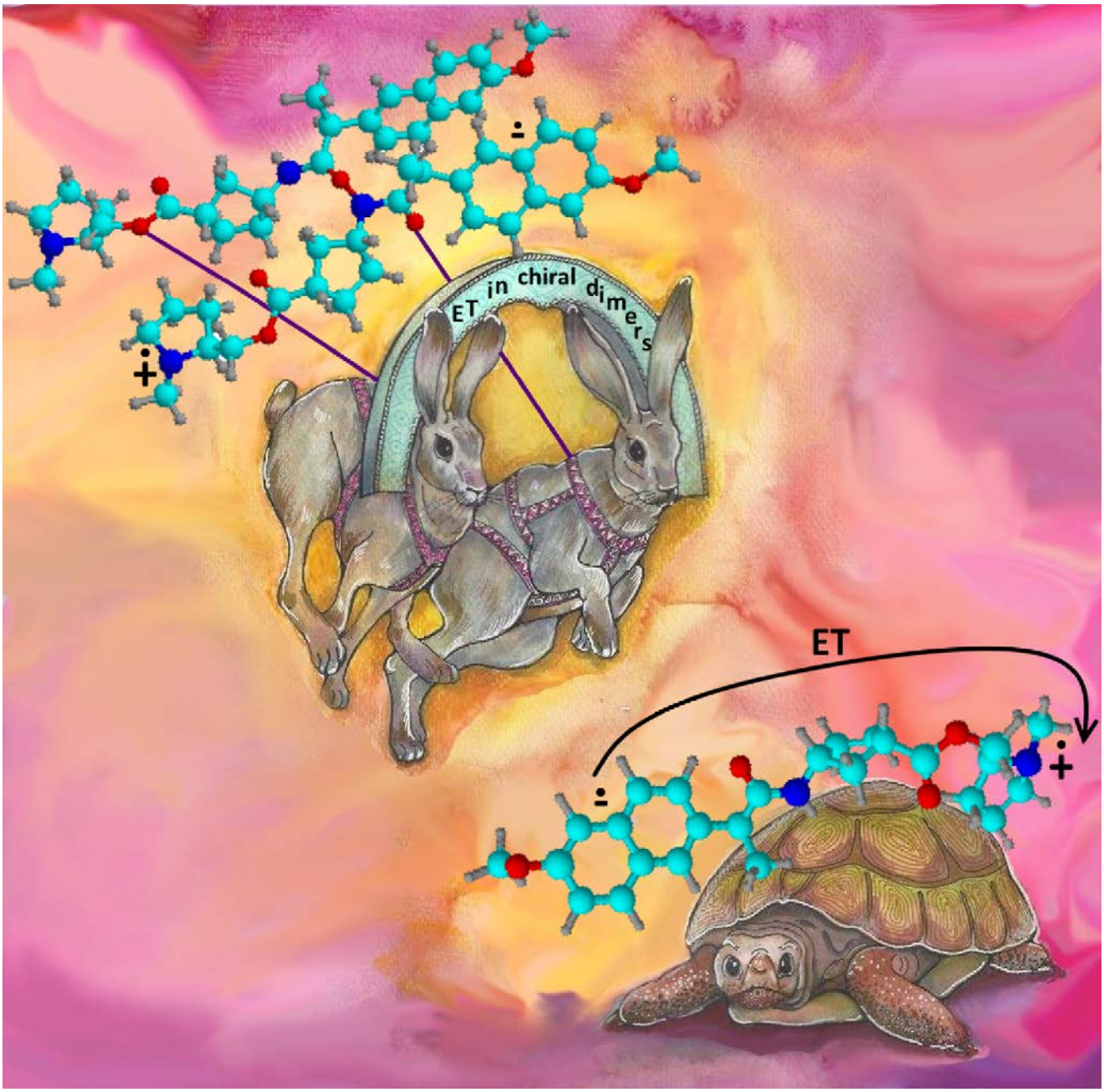

Abstract: The origin of biomolecules in the pre-biological period is still a matter of debate, as is the unclarified nature of the differences in enantiomer properties, especially the medically important activity of chiral drugs. On the first issue, significant progress has been made in the last decade of the 20th century with the experimental confirmation of Frank's popular theory on chiral catalysis in spontaneous asymmetric synthesis. Prof. Soai examined the chiral catalysis of the alkylation of achiral aldehydes by achiral reagents. Attempts to model this process have demonstrated the key role of chiral compounds associates as templates for chiral synthesis. However, the elementary mechanism of alkylation and the role of free radicals in this process are still incompletely understood. Meanwhile, the influence of external magnetic fields on chiral enrichment in the radical path of alkylation has been predicted. In addition, the role of chiral dyad association in another radical process - electron transfer (ET) - has been recently demonstrated by the following methods: chemically induced dynamic nuclear polarization (CIDNP), NMR, XRD and photochemistry. The CIDNP analysis of ET in two dyads has revealed a phenomenon first observed for chiral systems - spin selectivity, which results in the difference between the CIDNP enhancement coefficients of dyad diastereomers. These dyads are linked systems consisting of the widespread drug (*S*)-naproxen (NPX) or its (*R*)-analogue and electron donors, namely, (*S*)-tryptophan and (*S*)-*N*-methylpyrrolidine. Since NPX is one of the most striking examples of the difference in the therapeutic properties of enantiomers, the appearance of spin selectivity in dyads with (*S*)- and (*R*)-NPX and (*S*)–donors can shed light on the chemical nature of these differences. This review is devoted to discussing the chemical nature of spin selectivity and the role of chiral associates in the chiral catalysis of an elementary radical reaction – ET in chiral dyads.

1. Introduction

The origin of life in nature, from the chemical perspective, has two principal issues: the origin of chiral biomolecules and the physicochemical reasons for the differences in the biological and medical activity of enantiomers. These topics remain a matter of debate, despite many studies by researchers from various fields of science.[1,2] On account of the practical significance of chiral molecule synthesis, there are a number of theories, including the theory of spontaneous asymmetric synthesis in the presence of a chiral catalyst.[3] In this review, we will touch upon manifestations of chiral catalysis and discuss the genesis of the difference between enantiomers as a part of diastereomers – namely, between the chemically induced dynamic nuclear polarization (CIDNP) enhancement coefficients of electron transfer (ET) in donor-acceptor dyads. The phenomenon in question refers to the effects of spin selectivity.

The theory of spontaneous asymmetric synthesis occurring under the action of chiral catalysts is one of the most widely accepted among chemists.[3] This theory, proposed in 1953 by F. C. Frank, showed mathematically that a small amount of one chiral compound can increase its own reproduction and suppress the formation of another optical isomer in the reaction mixture. In this theory, the main requirement to obtain the prevalence of one isomer is the presence of a chiral associate, e.g., the presence of (*S,S*), (*R,R*) and (*R,S*) dimers. In Frank's conception, the driving force of chiral enrichment is the competition between the catalysing action of one enantiomer on the formation of the same isomer, occurring in (*S,S*) (or *R,R*) dimers, and the inhibition of the formation of another optical isomer as a part of an (*R,S*) dimer.

Brilliant experimental confirmations of this theory have been presented in a series of works by the Japanese researcher Kenso Soai.[4,5] He has obtained a high degree of enrichment of one enantiomer during the alkylation of various achiral aldehydes by diisopropylzinc in a non-chiral medium. Chiral catalysis resulted from the addition of a small quantity of the chiral product – alcohol – into the reaction mixture (see Scheme 1).

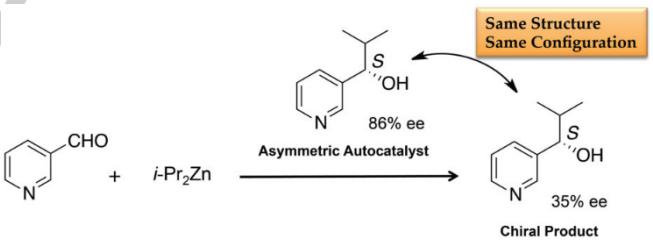

Scheme 1. Asymmetric autocatalysis of chiral pyridyl alkanol formation; first reported by K. Soai. Reproduced with permission from Ref. [5] © John Wiley & Sons, Ltd., 2014.

Since the publication of Soai's first results on chiral enrichment, numerous attempts to understand the mechanism of chiral catalysis have been made.[6-14] Particular attention has been paid to the quantum-chemical modelling of the reaction kinetics and the structures of associates formed in the reaction and to experimental confirmations of these associate structures. Modelling has been developed in the framework of Frank's theory. Schaffiano and Buono[7,8] first suggested the catalytic cycle model of the Soai reaction that was further developed

[a] A.A. Ageeva, Dr. E.A. Khramtsova, Dr. I.M. Magin, Prof. P.A. Purtov, Prof. T.V. Leshina
Laboratory of Magnetic Phenomena
Voevodsky Institute of Chemical Kinetics and Combustion SB RAS
Institutskaya 3, 630090 Novosibirsk (Russia)
E-mail: al.ageeva@gmail.com
[b] Dr. E.A. Khramtsova, Prof. P.A. Purtov
Novosibirsk State University
Pirogova 2, 630090 Novosibirsk (Russia)
[c] Prof. M.A. Miranda
Departamento de Química/Instituto de Tecnología Química UPV-CSIC, Universitat Politècnica de València, Camino de Vera s/n, 46022 Valencia (Spain)

afterwards by Gridnev and Vorobiev.[9,10] According to this model, during the alkylation of aldehydes, a chiral alcohol, acting as a catalyst, interacts with diisopropylzinc to form associates. The associates are imagined as dimers, tetramers and oligomers of zinc alcoholates (obtained from a chiral alcohol).[6-10] For example, one of the models considers a kinetic scheme in which two molecules of dialkylzinc react with two molecules of aldehyde to form a tetrameric product. Then, the latter dissociates, resulting in the regeneration of the catalyst and formation of the chiral alcohol, thereby providing chiral enrichment.[9]

Associates of diisopropylzinc alkoxide oligomers have recently been isolated, and their crystal structures have been studied by XRD at low temperature (see Figure 1).[6,15]

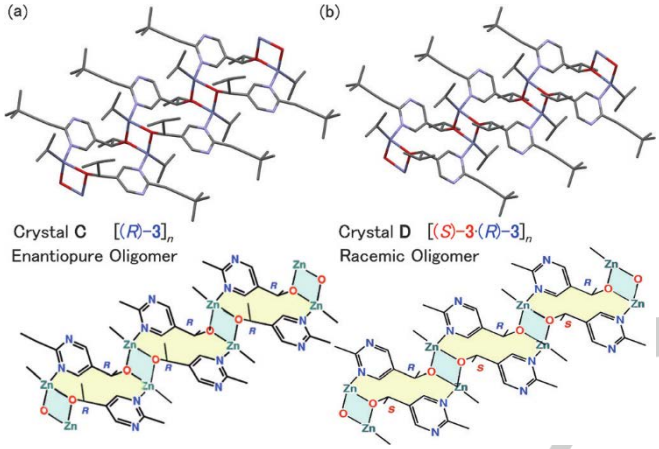

Figure 1. Single-crystal X-ray structures and simplified drawing of alkoxide oligomer crystallized with 1-2 equiv. iPr_2Zn. a) Enantiopure alkoxide oligomer crystal C. b) Racemic alkoxide oligomer crystal D. Reproduced with permission from Ref. [15] © John Wiley & Sons, Ltd., 2015.

Matsumoto and co-workers have shown that the structures of tetramers and oligomers obtained by using XRD in the solid state conform to the structures calculated in ref.[7-10] The currently available NMR data concerning the formation of associates in the Soai reaction, however, are very fragmentary and contradictory.[9,10]

In addition, the chiral catalysts of the Soai reaction have turned out to be a large number of other compounds (Table 1). Analysis of these data (Table 1) leads to the conclusion that the most essential condition of successful asymmetric synthesis is the ability of reagents to form associates that serve as templates or the presence of other compounds as templates in the reaction mixture.

In addition, there is no clarity regarding the details of the alkylation mechanism. The authors of the abovementioned models simply assumed by default that the alkylation process is a stereoselective transfer of the isopropyl group from diisopropylzinc to aldehyde. Nevertheless, there is a point of view according to which this transfer can occur in a radical pair.[16,17]

The work of Hegstrom and Kondepudi[18] simulated the chiral enrichment in the alkylation process within the framework of a radical mechanism. Scheme 2 presents the proposed radical mechanism, wherein the first stage (I) is the formation of a coordination complex of reagents. In stage II, according to the proposed mechanism,[18], this complex must be converted into a biradical or radical pair.

Table 1. Enantioselective iPr_2Zn addition to pyrimidine-5-carbaldehyde 2 initiated using chiral compounds followed by asymmetric autocatalysis. Reprinted with permission from Ref.[4] Copyright (2014) American Chemical Society.

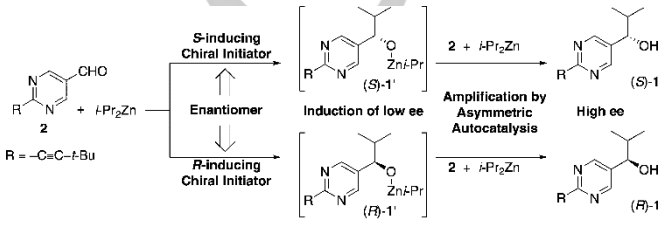

Entry	Chiral Initiator		5-Pyrimidyl Alkanol 1		Ref.
	Structure	Config.	Config.	ee (%)	
1		*S*	*S*	93	47
		R	*R*	96	
2		*S*	*S*	92	48
		R	*R*	90	
3		(1*S*,2*R*)	*S*	99	49,50
		(1*R*,2*S*)	*R*	99	
4	Helical silica	Right-handed	*S*	96	51
		Left-handed	*R*	97	
5	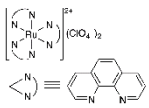	Δ	*S*	91	52
		Λ	*R*	88	
6	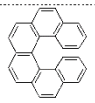	*P*	*S*	95	53
		M	*R*	95	
7	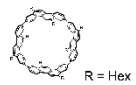 R = Hex	*M*	*S*	91	54
		P	*R*	91	
8	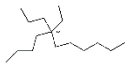	*R*	*S*	97	55
		S	*R*	97	
9		–	*S*	94	56
			R	92	

Although the authors of ref.[18] have not specified the structure of the biradical or radical pair, unpaired electron density can reasonably be assumed to be located at oxygen and metal atoms, as shown in Scheme 2 (stage II). Thus, the products of alkylation – chiral (*R*) and (*S*) alcohols – will be obtained via the radical mechanism. The resulting chiral

compounds, in turn, form associates called clusters, $(R\text{-}R)_n$ and $(S\text{-}S)_n$, that are catalysts (stages III, IV). However, the $(R\text{-}S)_n$ cluster has no catalytic activity (stage V). The interaction with a chiral catalyst results in the production of a chiral alcohol of the same configuration as the catalyst (VI, VII). The repetition of stages V-VII increases the initially small predominance of one enantiomer.

The production of one enantiomer excess in the reaction of prochiral reagents is well known to be achieved under the action of physical factors as well, such as CPL, magnetic and electric fields.[1]

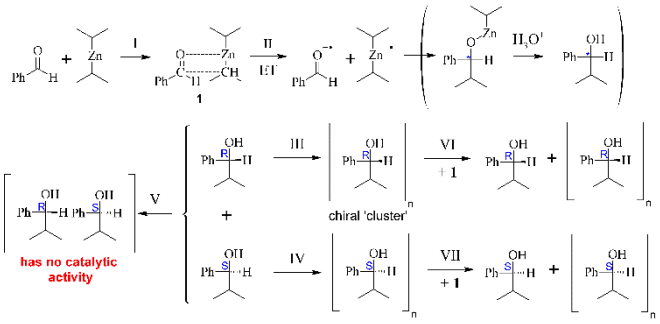

Scheme 2. Mechanism of chiral catalysis (adapted from[18]).

In this regard, the work[18] aims to demonstrate one of the physical factors leading to chiral enrichment – an external magnetic field (EMF). The next picture shows the influence of an EMF on the chiral enrichment efficiency of the radical process (Figure 2). This additional factor affects the limiting radical stage (I) of Scheme 2, increasing the chiral product content as the magnetic field strength increases. The dependence of chiral enrichment on magnetic field strength presented in Figure 2 has been calculated in the framework of so-called radical pair theory (RPT).[19] This theory refers to the field of spin chemistry describing, in particular, patterns of radical reactions.

Thus, the results of the work of Soai[4,5] and further numerical calculations[6-11,18] have shown that the participation of chiral compound associates as catalysts in the ionic and radical reactions of achiral reagents can result in an excess of chiral products.

However, a very large set of compounds with widely different structures are capable of catalysing chiral enrichment in the Soai reaction, which indicates a lack of understanding of the nature of this catalysis.[20] Clearly, the assumption of a single mechanism, where – an associate of chiral compounds – acts as a catalyst by serving as a chiral template, is not enough. In this regard, the discovery of other chiral catalysed reactions with established mechanisms would be desirable.

As a matter of fact, chiral catalysis has recently been experimentally detected in the elementary process of ET, occurring in donor-acceptor chiral dyads.[21] Two dyads have demonstrated a new peculiarity of chiral systems – spin selectivity of ET. Spin selectivity manifests itself as a difference in the CIDNP enhancement coefficients of the (*R,S*) and (*S,S*) dyad diastereomers.[21] Since the effects of CIDNP, formed under the UV irradiation of diastereomer mixtures, correlate with dimer concentrations ((*R,S*)–(*R,S*), (*S,S*)–(*S,S*) and (*R,S*)–(*S,S*)), ET might be considered another example of chiral catalysis.

The source of spin selectivity has been shown to be the difference in magnetic resonance parameters, namely, the hyperfine interaction constants in the paramagnetic forms of the (*R,S*) and (*S,S*) diastereomers. These paramagnetic particles are formed via intramolecular photoinduced ET in dimers of dyads.[21-24]

The newly observed spin selectivity of ET in diastereomers of donor-acceptor dyads is worthy of attention for several reasons. First, chiral radicals have been insufficiently investigated. Second, another crucial problem of chiral compounds is the undiscovered nature of differences in the medicinal activities of drug molecule enantiomers.[2] The dyads studied are linked systems consisting of a well-known nonsteroidal anti-inflammatory drug (NSAID), (S)-naproxen (NPX), and its (R) analogue amide derivatives. Note that (R)-NPX is not an NSAID at all. The electron donors in these dyads are the residues (S)-N-methylpyrrolidine and (S)-tryptophan (Trp) (Figure 3).

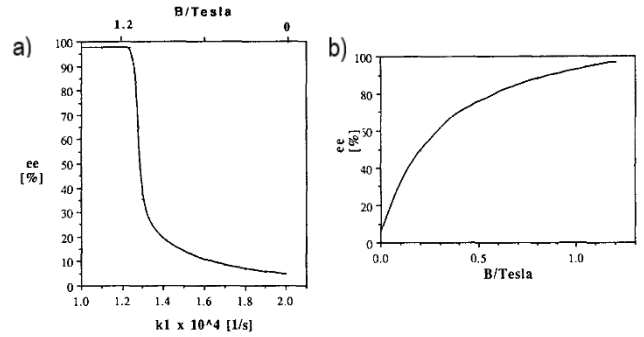

Figure 2. Dependence of enantiomeric enrichment (ee): a) on the rate constant k_1 corresponding to stage II in Scheme 2, b) on the magnetic field strength calculated according to Scheme 2. Reprinted from Ref. [18], Copyright (1996), with permission from Elsevier.

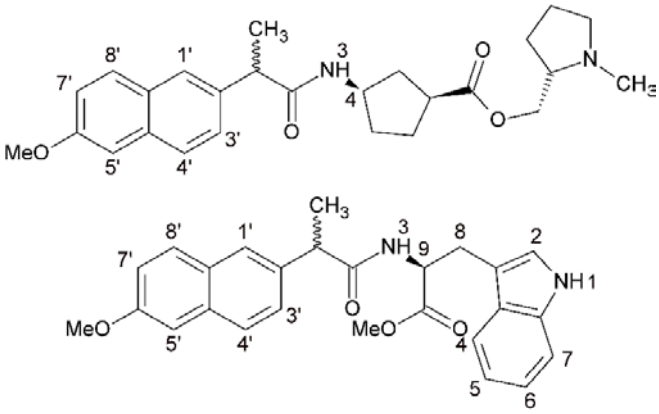

Figure 3. Molecular structure of dyad **1** (top) and **2** (bottom). Reproduced with permission from Ref. [21] © John Wiley & Sons, Ltd., 2018.

The donor-acceptor interaction in these dyads can be considered as a model of drug-enzymes binding.[21] In turn, the spin selectivity of ET in diastereomers with (*S*)- and (*R*)-NPX suggests some difference in the oxidation-reduction properties of enantiomers as a part of diastereomers. Thus, this report focuses on two issues: the chemical nature of ET spin selectivity in chiral dyads and the chiral catalysis of this process.

2. Spin selectivity of ET in dyads with (*S*)- and (*R*)-NPX

The choice of studied systems is because NPX is one of the most well-known and widely studied NSAIDs in which optical isomers exhibit different biological activity.[2,25,26] (*S*)- and (*R*)-NPX differ in anti-inflammatory activity (the drug is only (*S*)) and propensity to chiral inversion (only (*R*) undergoes it). In addition, (*R*) is more efficiently metabolized by cytochrome P 450[27] and inhibits cannabinoid oxidation.[26] To establish the causes of abovementioned differences in the properties of the optical isomers, ref.[22] proposed an original approach. The reactivity of (*R*)- and (*S*)-NPX was studied in model systems consisting of donor-acceptor dyads with a second chiral centre. The systems used in the investigation are presented in Figure 3. There are physical prerequisites for the differences in the reactivity of the (*R,S*) and (*S,S*) diastereomers in these dyads. In living organisms, when NPX binds with the active sites of enzymes COX 1 and 2, the drug molecule interacts with chiral amino acid residues.

Under the UV irradiation of dyads **1** and **2,** a local excited state of NPX was shown to be formed. Photochemistry and spin chemistry studies have shown that the quenching of the NPX excited singlet state involves intramolecular ET accompanied by the formation of a biradical zwitterion (BZ) (see Figure 4).[21-23]

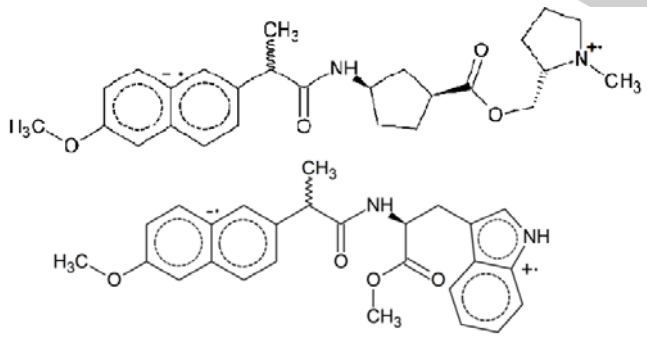

Figure 4. Biradical zwitterions (BZs) of dyads **1** and **2**.

In the case of dyad **1,** the quenching of the excited state by an *N*-methylpyrrolidine fragment is described in Scheme 3. Stages k_1-k_5 in this scheme were established by fluorescence kinetics analysis, whereas the formation of BZ was detected by the CIDNP method.[22]

The quenching of the NPX excited state in dyad **2** under the action of a tryptophan moiety occurs according to Scheme 4. Note that in both cases, the rate constants for the *(R,S)* and *(S,S)* diastereomers of dyads **1** and **2** are different.[22,23]

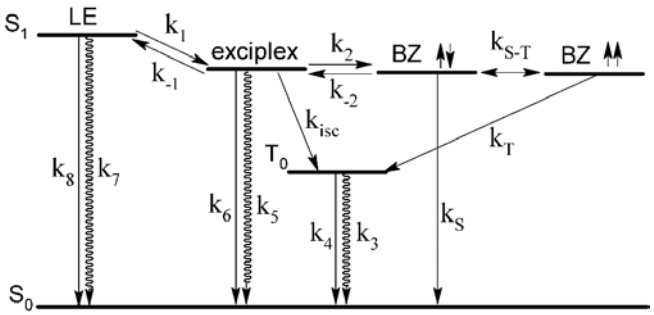

Scheme 3. Quenching mechanism of the NPX local excited state (LE) of dyad **1**: k_1 and k_{-1} – rate constants of the transformation of LE into exciplex and exciplex to LE; k_2 – ET rate constant; k_{-2} – rate constant of BZ to exciplex back transfer; $k_{S\text{-}T}$ – spin conversion constant in BZ; k_S and k_T – rate constants of back ET from singlet and triplet spin states of BZ, respectively; k_3 and k_4 - rate constants of triplet non-radiative and radiative decay; k_6 and k_8 – fluorescence constants; and k_5 and k_7 – constants of non-radiative decay of LE and exciplex; $k_{isc\ (exc)}$ – internal conversion constant in exciplex.

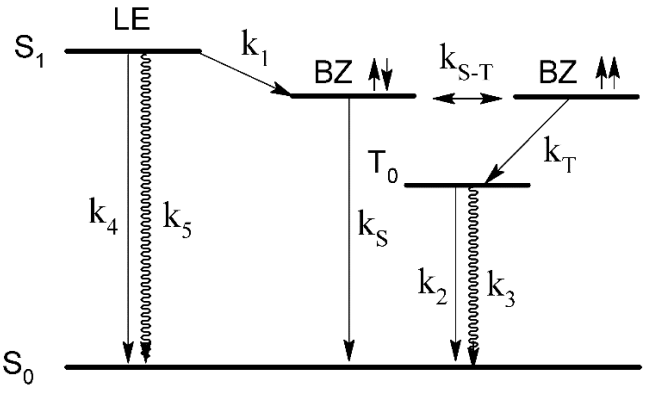

Scheme 4. Quenching mechanism of the NPX local excited state (LE) of dyad **2**: k_1 – ET rate constant; $k_{S\text{-}T}$ – spin conversion constant in BZ; k_S and k_T – rate constants of back ET from singlet and triplet spin states of BZ, respectively; k_2 and k_3 – rate constants of triplet radiative and non-radiative decay, k_4 and k_5 – fluorescence constant and non-radiative decay constant of LE.

The CIDNP phenomenon is the manifestation in NMR spectra of the products of radical reactions as signals of nuclei with the spin state populations different from the Boltzmann. The phases (emission or enhanced absorption) and intensities of these signals depend on certain parameters, such as hyperfine interaction (HFI) constants, the difference in g-factors of partners in a radical pair (RP) or biradical, the multiplicity of RP precursors, and a few more parameters.[19] In essence, CIDNP effects reflect the difference in the recombination probability of RPs with α_N and β_N nuclear spin projections on the magnetic field direction (Figure 5).

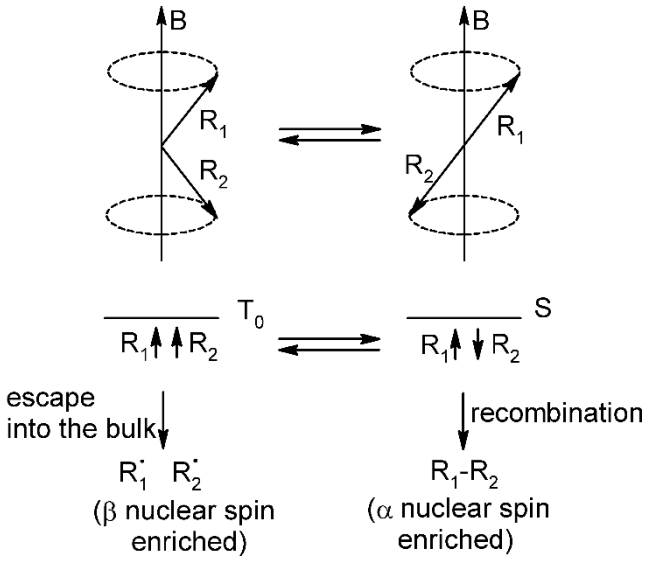

Figure 5. Vector model of the singlet – triplet evolution of an RP in a triplet (T_0) state in a high magnetic field. The model depicts transitions between unreactive triplet and reactive singlet collective spin states of RP. S-T_0 transitions are induced by the difference in the Larmor precession frequencies of R_1 and R_2, in accordance with equation (1).

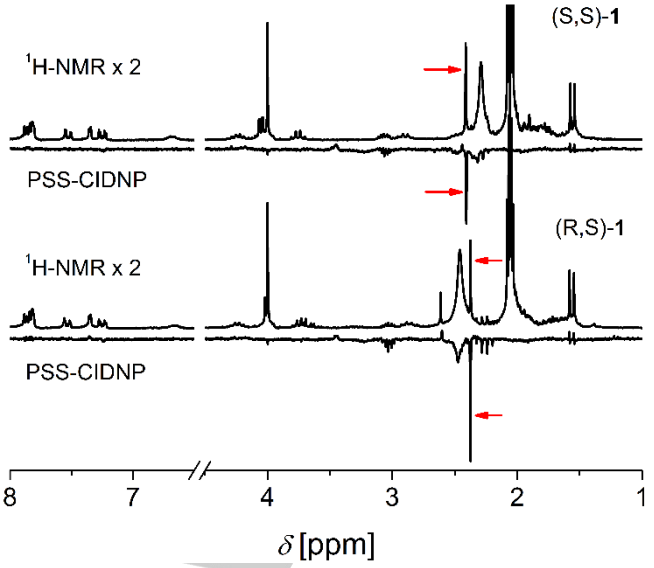

Figure 6. NMR and pseudo-steady-state (PSS) CIDNP spectra of dyad **1** diastereomer (5 mM) solution in CD_3CN (H_2O 0.05%): (*S,S*) - top, (*R,S*) - bottom. The negative polarized line at 2.3 ppm (red arrows) corresponds to the methyl protons of the *N*-methylpyrrolidine fragment of the dyad diastereomers. Reproduced with permission from Ref. [21] © John Wiley & Sons, Ltd., 2018.

The source of this difference is the difference in the energy of electron-nuclear interaction in RPs and in the Larmor precession frequencies of radical partners. For the simplest case of an RP with a single magnetic nucleus, these interactions are represented by the following Hamiltonian:

$$\hat{H} = g_1\beta B\hat{S}_{1z} + g_2\beta B\hat{S}_{2z} + a\hat{S}_1\hat{I} \quad (1)$$

where g_1, g_2 are g-factors of electrons, S_1, S_2 are electron spins of partners of RP (R_1, R_2), β is the Bohr magneton, B is the induction of an EMF, and a is the HFI constant between the electron and nuclear spins in the radical centre R_1.

Thus, CIDNP analysis provides information about the distribution of spin density in the paramagnetic precursors of polarized products and therefore about the structures of these precursors. This information on the spin density distribution in the paramagnetic forms of drug molecules can be practically significant for the binding of a drug with receptors or enzymes, if this binding involves stages with charge transfer.

The CIDNP spectra of the studied systems – the (*R,S*) and (*S,S*) configurations of both dyads – are presented in Figures 6 and 7.

The CIDNP effects observed at the protons of the (*R,S*) and (*S,S*) configurations of both dyads under UV irradiation indicate ET. Intramolecular ET was proved by investigation of the dependence of CIDNP effectivity on dyad concentration.

The above implies that the intensities of the polarized lines in CIDNP spectra in general should be proportional to the HFI constant values of the corresponding nuclei in the radical precursors. However, with large differences in the HFI constants of different nuclei, the contribution to spin evolution from the nucleus with the highest constant will prevail. Then, the chemical polarization of this nucleus alone can be observed.

Actually, this situation takes place in dyad **1**: the HFI constants of the methyl protons in the *N*-methylpyrrolidine fragment and of the aromatic protons in NPX are 2.9 mT and 0.5 mT.[23,24] The resulting CIDNP of these methyl protons alone is presented in Figure 6. In addition, there is a difference in CIDNP intensity between the (*R,S*) and (*S,S*) diastereomers. To quantify the CIDNP effects of the diastereomers, enhancement coefficients will be used as determined below.

The CIDNP enhancement coefficient for one RP is equal to the intensity of the polarized proton signal (I_{pol}) divided by the equilibrium intensity of the signal in the NMR spectrum (I_{eq}) and the concentration of [*BZ*]. For convenience, we will use the ratio of CIDNP enhancement coefficients derived from[21]

$$K = \frac{I_{pol}^{RS} \times I_{eq}^{SS} \times [BZ]_{SS}}{I_{eq}^{RS} \times I_{pol}^{SS} \times [BZ]_{RS}} \quad (2)$$

where [*BZ*] is determined by

$$[BZ] = (1 - 10^{-A}) \frac{\lambda E (1 - \varphi_{fl})}{hcN_A V} \quad (3)$$

where A is the absorption of a 5 mM solution of dyads at 308 nm; λ is the wavelength of the laser light; E is the energy of the incident laser light; φ_{fl} are the fluorescence quantum yields of the studied dyads; V is the irradiated volume fraction of the sample; N_A is Avogadro's constant; h is Plank's constant; and c is the speed of light.

Therefore, the ratio of enhancement coefficients for the CH_3 protons of the (*R,S*) and (*S,S*) diastereomers of dyad **1**, according to equation (2), is equal to 2.3 ± 0.1.

In the CIDNP spectra of dyad **2**, differences between several lines belonging to the (*R,S*) and (*S,S*) diastereomers are observed (Figure 7).

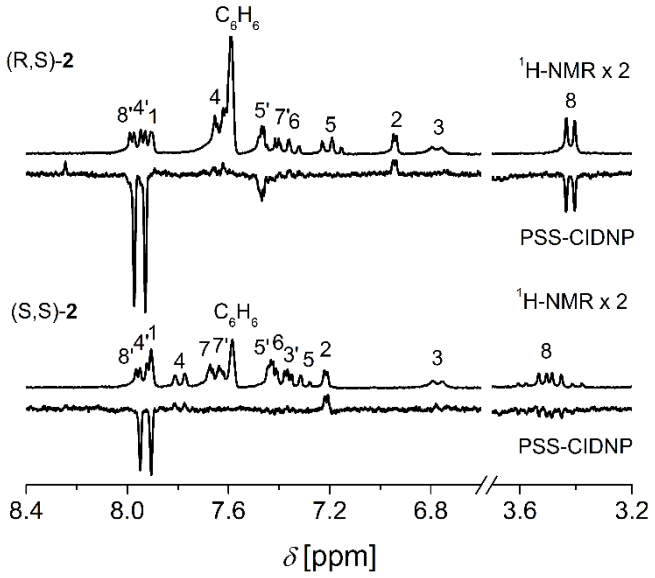

Figure 7. NMR and pseudo-steady-state (PSS) CIDNP spectra of dyad **2** solutions (5 mM in 40% C_6D_6, 0.17% H_2O, the rest is CD_3CN): (*R,S*) - top, (*S,S*) - bottom. Reproduced with permission from Ref. [21] © John Wiley & Sons, Ltd., 2018.

In this system, there is not such a large difference between the HFI constants in the BZ as in the case of dyad **1**. Therefore, CIDNP is observed on several types of protons. The HFI constants of the NPX aromatic protons at the 8' position and of the CH_2 group of Trp are 0.5 mT and 0.7-1.0 mT, and the HFI constants of the indole protons have values of the same order as those of NPX.[23]

The analysis of the CIDNP effects also confirms the reversible ET in dyad **2**. If we compare the CIDNP effectivity ratios of different protons in this dyad, as in the example of the (*R,S*) diastereomer, with the ratios of the corresponding HFI constants, we will see that the average ratios in the time-resolved spectra of NPX and β-CH_2 protons correspond to the spin density distribution in the BZ.[23] As indicated in Figure 7, the (*R,S*) configuration of NPX has greater polarization of the protons at the 8'(4') and 5' positions than the (*S,S*) diastereomer. In the (*S,S*) configuration, the polarized signal of the 5' proton is absent. Moreover, there is a clear-cut distinction between the CH_2 protons (8 position) in the NMR and CIDNP spectra. The latter may be closely related to the secondary processes of dyad decay via neutral biradical. Therefore, the CIDNP spectrum is the superposition of polarized protons from the BZ and the neutral biradical.[23]

For this dyad, the maximal ratio of CIDNP enhancement coefficients of (*R,S*) and (*S,S*) diastereomers is also two, but in general, this value depends on the solvent. This relationship will be discussed in the next section.

The dependence of CIDNP effectivity on the solvent permittivity of dyad **1** and **2** has been studied in previous works.[22,23] Analysis of these dependencies for the diastereomers of dyad **1** allows tracing of the relationship between CIDNP effectivity and the quantum yields of exciplexes.[22] The equilibrium between the exciplex and BZ is completely shifted to the BZ side in acetonitrile. In this case, the influence of this equilibrium on the CIDNP coefficient is minimal. Therefore, to study the nature of the difference in CIDNP enhancement coefficients of the diastereomers of dyad **1,** the authors of ref.[21] compared enhancement coefficients measured only in acetonitrile. In the polar environment, the main contribution to CIDNP is assumed to derive from the magneto-resonance parameters of the BZ. The ratio of these coefficients for (*R,S*) and (*S,S*) diastereomers has been compared with the value calculated in the framework of RPT.[19] The goal of this comparison was to determine what difference in BZ parameters is required to ensure a twofold difference in CIDNP coefficients.

The CIDNP effects of the diastereomers of dyad **1** were first calculated in ref.[22] by numerical simulation of the dependence of CIDNP on solvent permittivity, developed in accordance with Scheme 1. The calculation was performed in the framework of a simple two-position model[22], where systems can be in the reaction zone with a limited thickness of the reaction layer or out of the reaction zone. The model also considers spin evolution in the BZs, occurring in the Coulomb field. To calculate the recombination probability, the Liouville approximation was applied with variation in the diffusion coefficients and the thickness of the reaction layer. The BZ lifetime was set to 10^{-7} s for both diastereomers. The calculation was also carried out considering the recombination from both collective spin states of the BZ (with k_S and k_T rate constants). The change in the ratio of these constants in media with different permittivity determines the shape of the dependences.[21]

The above model coincided well with the experimental data, except in the region of high polarity (Figure 8).

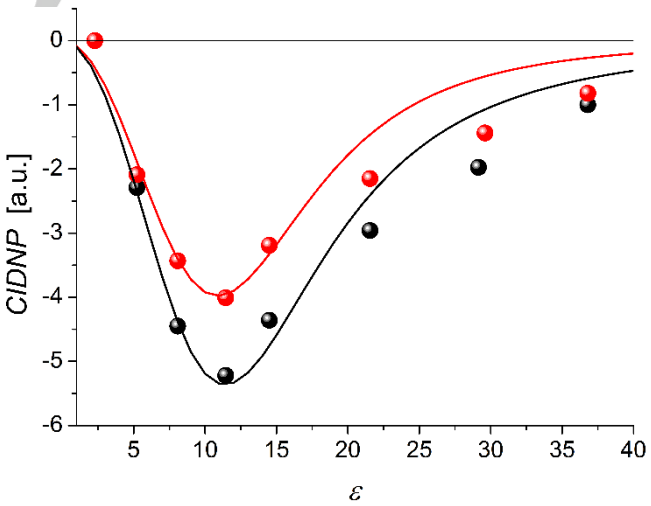

Figure 8. Dependence of CIDNP effects on the solvent dielectric constant for dyad **1**: (R,S) - black balls, (S,S) – red balls. The solid lines are calculated dependences. Reproduced from Ref. [22] with permission from the PCCP Owner Societies.

Therefore, the calculation of CIDNP in the solvents with high dielectric constants was carried out in ref.[21] using a two-

position model but excluding Coulomb interaction and with variation in the magnetic resonance parameters and the lifetimes of the BZs. The recombination probability - the back ET in the BZs - was calculated using the Green function method in accordance with Scheme 1. For the reasons stated above, the simplified reaction scheme excluding the exciplex was used in ref.[21] Thus, the following constants were equal to zero: the rate constants of the transformation of the LE into the exciplex and of the exciplex into the LE (k_1 and k_{-1}), the rate constant of exciplex transfer into the BZ and BZ back transfer into the exciplex (k_2 and k_{-2}) and the rate constant of internal conversion in the exciplex ($k_{inc\ (exc)}$).

The rate constants k_S and k_T are considered to be close for the case of recombination from singlet and triplet BZ spin states.[21] To calculate the recombination probability within the framework of a two-position model, reaction times must be determined: the overall system lifetime is τ_c, and the total time the system is in the reaction zone is τ_r. The initial spin state of the BZ is singlet, while the reactive state might be singlet or triplet. The definition of the recombination probability implies finding τ_S, the total time the BZ is in the reaction zone in reactive singlet state. All details of the calculation are given in ref.[21]

The results of the calculation of the dependence of the CIDNP coefficients for dyad **1** diastereomers on HFI values with simultaneous variation of the Δg values and the characteristic times τ_c are presented below (Figures 9, 10).

The experimental difference in the CIDNP coefficients will correspond to a twofold change in HFI constants with the following set of parameters: τ_c = 10 ns (whereas the experimental values are 7 and 9 ns for the (*R,S*) and (*S,S*) diastereomers of dyad **1**), τ_r = 1 ns and $\Delta g = 10^{-3}$.[22] The latter is also the experimental value.[24]

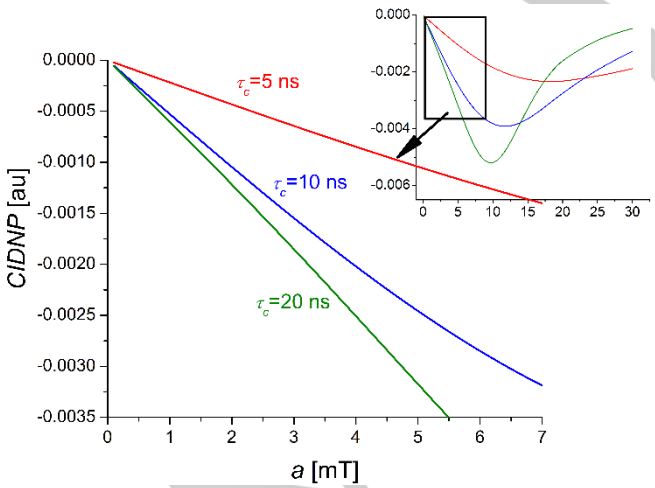

Figure 9. Starting points and full curves (in insert) of the CIDNP intensity dependences on HFI constant values for B = 4.7 T, τ_c = 10 ns, τ_r = 1 ns and various Δg. Reproduced with permission from Ref.[21] © John Wiley & Sons, Ltd., 2018.

A similar result can be obtained by varying the Δg values from 0.001 to 0.002. Note that such significant changes in the values of the *g*-factor can be expected only in the case of additional changes in the structure of BZ.

Indeed, to describe the differences in the CIDNP coefficients of diastereomers, the same twofold or greater difference between the BZ lifetimes is required: for example, increasing τ_c from 5 ns to 10-20 ns for the (*R,S*) and (*S,S*) configurations, respectively (Figure 10).

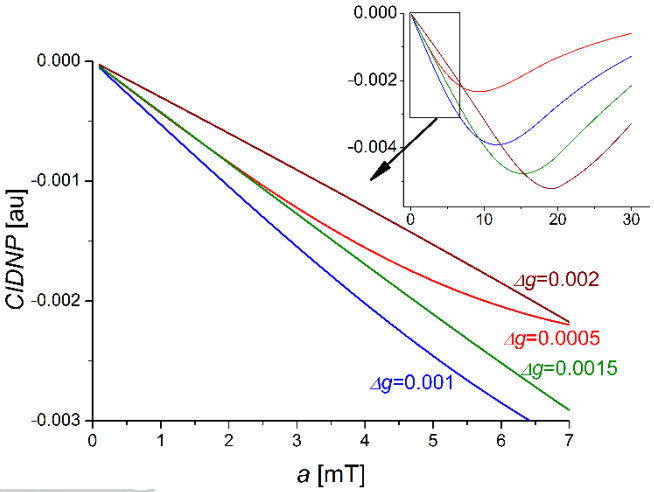

Figure 10. Starting points and full curves (in insert) of the CIDNP intensity dependences on HFI constant values for B = 4.7 T, τ_r = 1 ns, Δg = *0.001* and various τ_c. Reproduced with permission from Ref.[21] © John Wiley & Sons, Ltd., 2018.

Meanwhile, as mentioned above, BZ lifetimes (τ_c) of the dyad **1** diastereomers in acetonitrile differ much less: from 9 to 7 ns.

Regarding the variations in τ_r, as explored in ref.[22], the change in the thickness of the reaction zone was shown not to improve the consistency with experimental results in the region of high polarity (Figure 8).

Therefore, the above results reveal that twofold changes in CIDNP coefficients occur under for similar variations of BZ parameters (HFI, g-factors, τ_c). The most likely reason for the differences in the CIDNP of the diastereomers seems to be the difference in their HFI constants. This conclusion, drawn in ref.[21], is based not only on the results of calculations but also on analysis of the reference data.[28 -32] According to the EPR data, a twofold difference between the HFI constants of optically active stable radicals and biradicals in solid state and solution had already been observed. For g-factors, appreciably smaller changes were observed.[30-32]

The authors of ref.[21] confined themselves to calculating CIDNP in the diastereomers of dyad **1**, since the chosen single-nucleus approximation allows the evaluation of CIDNP only for a nucleus with a maximum HFI constant in the RP. The CIDNP pattern in dyad **2** did not satisfy this condition. However, there is

no doubt that the revealed trends also applied to the second dyad.

Thus, the results of this section have demonstrated the spin selectivity of back ET in short–lived paramagnetic forms of dyads with (*S*) and (*R*)-NPX, thereby indicating that the difference in HFI constant is a new peculiarity of the NPX enantiomers as a part of diastereomers.

Further, we will make an effort to trace the possible relation between spin selectivity and chiral enrichment. Note that the difference in the CIDNP coefficients of diastereomers also means a difference in the recombination probability in a pair of paramagnetic precursors. Then, if the formation of a chiral product occurs through the stage of singlet-triplet conversion, some enrichment of the reaction mixture with an optical isomer having a higher HFI constant can be expected.

Therefore, the initial enrichment during the pre-biological period could be assumed to occur due to the magnetic field effect, provided the chiral compounds were obtained in radical reactions. As stated above, there is a considerable probability that the Soai reaction also involves radical stages.[16-18]

In the conclusion of this section, the fact that the chiral-induced spin selectivity effect (CISS) was described earlier in spintronics must be mentioned.[33] In this case, the CISS is the difference in the velocities of ET through charged films formed by compounds with spiral structure and different optical configurations. The CISS is explained by the difference in the energy of the spin-orbital coupling (SOC) of electrons in the media involving (*R*) and (*S*) enantiomers and is considered to be the result of the induction in charged media of electric and magnetic fields with different handedness and different direction. To describe the scale of the experimental CISS effects requires the assumption that the SOC values in chiral media are orders of magnitude greater than the usual ones for light atoms in organic compounds.[33]

3. The relationship between spin selectivity and dyad association

To study the chemical nature of the difference in CIDNP effects in dyad diastereomers, in ref.[21], the ratio of CIDNP enhancement coefficients measured in mixtures of dyad **1** diastereomers was also analysed. The mixtures consisted of different ratios of the (*R,S*) and (*S,S*) configurations in acetonitrile. An example of the CIDNP spectra detected under the UV irradiation of such a mixture is presented in Figure 11.

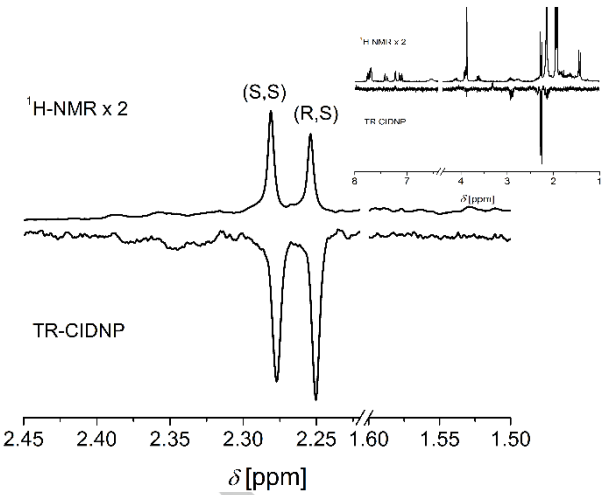

Figure 11. NMR and time-resolved (TR) CIDNP spectra of methyl protons area (full spectra are presented in insert) detected in the mixture of dyad **1** diastereomers in acetonitrile (the ratio of (*R,S*)-/(*S,S*)- = 0.8). Reproduced with permission from Ref.[21] © John Wiley & Sons, Ltd., 2018.

Note that the extinction coefficients of the dyad's diastereomers at λ = 308 nm were practically equal for both dyads: *(R,S)*-**1** and (*S,S*)-**1** ε = 840 ± 10 $M^{-1}cm^{-1}$; *(R,S)*-**2** and (*S,S*)-**2** ε = 850 ± 10 $M^{-1}cm^{-1}$. This fact means that the yields of diastereomers in excited states formed under UV irradiation will be proportional to the ratio of diastereomer concentrations. Below, Table 2 presents the ***K*** values obtained from CIDNP spectra with different diastereomer ratios.

Table 2. ***K*** values of dyad **1** diastereomers (column 2) determined for different ratios of diastereomer concentrations (column 1). Reproduced with permission from Ref.[21] © John Wiley & Sons, Ltd., 2018.

Ratio of (*R,S*)/(*S,S*) concentrations	***K***
0.4	1.70 ± 0.09
0.7	1.80 ± 0.09
0.8	1.80 ± 0.09
1.0	1.9 ± 0.1
1.3	2.0 ± 0.1
1.8	2.3 ± 0.1
2.1	2.3 ± 0.1
2.3	2.3 ± 0.1

The change in ***K*** values depending on the ratio of diastereomer concentrations shows that some intermolecular processes influence CIDNP formation. As suggested in ref.[21], this observation could be the manifestation of the association of diastereomers, most likely dimer formation.

In support of this conclusion, in the review, we will provide literature data on the association capabilities of the systems studied and the solvents used. Further experimental evidence of the association of dyads **1** and **2** will be presented.

A number of important processes involving the participation of chiral molecules, such as recognition and selection, are dependent on the concentrations of reagents.[34-36] In particular, polymerization accompanied by enrichment of one enantiomer shows such concentration dependence.[35,36] All these processes are believed to include the association of chiral molecules via the formation of hydrogen bonds as well as other weak interactions (e.g., van der Waals and dipole–dipole interactions). The association of substituted naphthalenes is generally considered to occur through the interaction of aromatic rings, and in the case of NPX, strong hydrogen bonds (H–bonds) are formed by acid residues.[37-39]

H-bonds are observed in the liquid and solid states of naphthalene and NPX, and they are retained even in dilute solutions.[40] There are reference data on the formation of dimers and excimers of substituted naphthalenes and NPX in solution.[38, 39] The association of NPX with biomolecules was also recorded using solid-state NMR and XRD[41] and shown to occur due to the formation of H-bonds between the carboxyl group of NPX and the NH and OH protons of biomolecules (amino acids and others).[41]

Since both studied dyads have amide groups, and dyad **2** also has an indole ring, association can be expected to occur mainly with the participation of these fragments. The H–bond between carbonyl from the amide group of one molecule and the NH proton from the other molecule of dyad **2** has been observed using single-crystal XRD at room temperature.[21]

The interactions between amide groups and aromatic rings in dyads and solvents also should not be neglected. Indeed, there are reference data showing the detection of weak collision complexes between amide groups and indole rings of various compounds in aromatic hydrocarbon solvents by NMR and optical methods.[42-44]

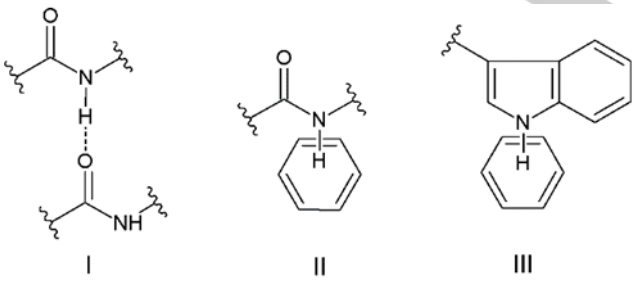

Figure 12. Amide group self-association (I) and collision complexes (II and III) of dyads with aromatic solvents. Reproduced with permission from Ref. [21] © John Wiley & Sons, Ltd., 2018.

To verify the presence of associates and collision complexes between diastereomers of dyads and between dyads and solvents, as depicted in Figure 12, NMR spectra were analysed.[21] The solutions were the same as those in which the CIDNP enhancement coefficients were measured. The chemical shifts and line widths in the NMR spectra of the solutions of dyads **1** and **2** have been analysed in detail in ref.[21]

In particular, researchers have assumed that solvation affects the values of ***K*** for the dyad **2**. Since no exciplexes are formed during the photolysis of this dyad, in accordance with Scheme 2, the ratios of the CIDNP enhancement coefficients were measured in different solutions of deuteroacetonitrile/deuterobenzene/water. The smallest ratio, ***K*** = 1.4, was observed in acetonitrile (0.2% water), and the ratio increased to 2 when up to 40% (volume fraction) C_6D_6 was added to the dyad solution. This difference might result from competition between dyad dimerization via the amide group in acetonitrile and the formation of its complexes with benzene.[42] If these processes occur with different efficiencies for the (*R,S*) and (*S,S*) diastereomers, different changes in the CIDNP coefficients should occur. The latter, in turn, will make ***K*** dependent on the solvent. This dependence might be a consequence of the different influence of solvation on the BZ conformations of (*R,S*) and (*S,S*) diastereomers and the corresponding differences in back ET efficiency.

In addition to the changes in the values of ***K*** in dyad **2**, significant changes in the chemical shifts of both dyads' protons were observed depending on the composition of the solution, in addition to broadening of NH proton lines (Figures 13-14).[21]

The change in the chemical shifts of the aromatic and aliphatic protons of both dyads depending on the concentrations of water and benzene in the solution indicate contributions of the solvation effect to the chemical shifts (Figure 13).

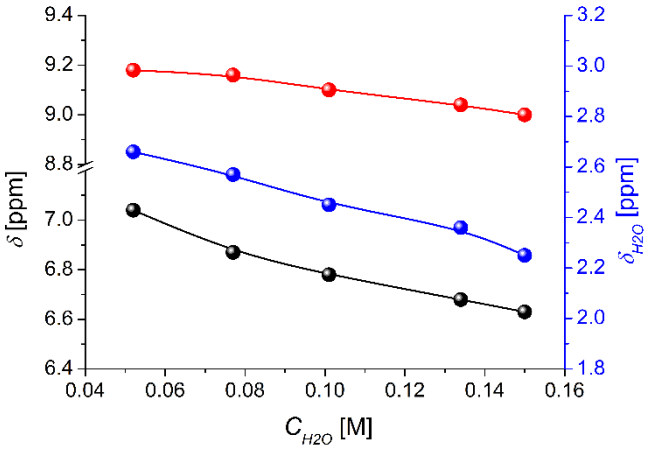

Figure 13. Dependences of the chemical shifts of NH(1) (red), NH(3) (black) and H_2O (blue) protons of the (*R,S*)-**2** dyad (10^{-3} M) on the water concentration in the mixture of $CD_3CN/C_6D_6/H_2O$. Reproduced with permission from Ref.[21] © John Wiley & Sons, Ltd., 2018.

Similar to changes in other chemical shifts, the change in the chemical shift of the water itself serves as an additional indication of its participation in the solvation process (Figure 13).

In addition, analysis of the line widths of amide group NH(3) protons of both dyads showed that the selective broadening (Figure 14) is due to slow proton exchange between the monomers and dimers of the dyads (Scheme 4, the first equilibrium) and to the solvation of dyads via H-bond formation (Scheme 4, second equilibrium).

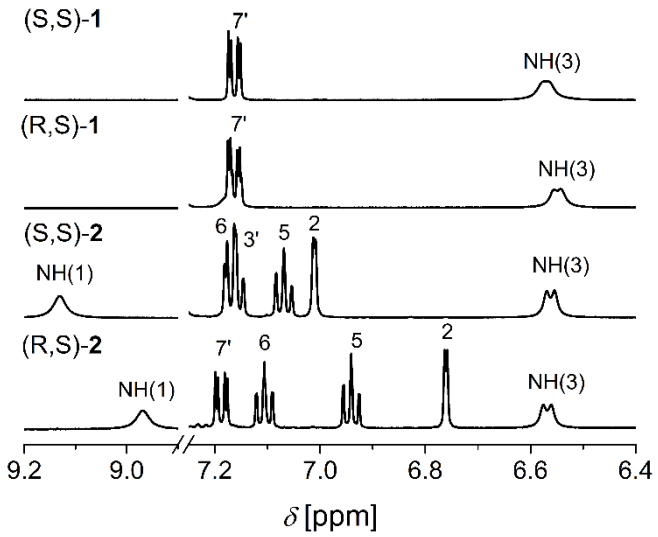

Figure 14. NMR spectra of aromatic protons in (*R,S*)-/(*S,S*)-**2** and (*R,S*)-/(*S,S*)-**1** dyads in the solvent mixture: CD_3CN + 0.17% H_2O. Reproduced with permission from Ref.[21] © John Wiley & Sons, Ltd., 2018.

As follows from Scheme 4, the dimers are formed due to H-bond formation between the carbonyl group of one molecule and the NH proton of the amide group of another.

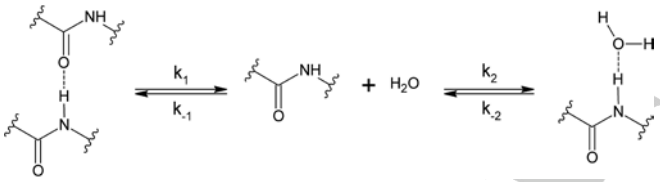

Scheme 4. The possible mechanisms of participation of the amide fragment of the studied dyads in H-bond formation. Reproduced with permission from Ref.[21] © John Wiley & Sons, Ltd., 2018.

Thus, the analysis of NMR data in solution for both dyads and of XRD of dyad **2** in the solid state has confirmed the possibility of the formation of dimers of dyad diastereomers and the formation of weak collisional complexes with solvents.

4. Calculation of CIDNP enhancement coefficient ratios depending on dimer concentrations

An attempt was also made to estimate the impact of dyad self-association on the CIDNP enhancement coefficient.[21] The calculations were carried out in the context of Frank's theory, taking into account that CIDNP occurs in both homodimers ((*R,S*)-(*R,S*) and (*S,S*)-(*S,S*)) and heterodimers ((*R,S*)-(*S,S*)) (Scheme 5).

$$RS + RS \underset{K_{RS}^-}{\overset{K_{RS}^+}{\rightleftharpoons}} D_{RS,RS}$$

$$SS + SS \underset{K_{SS}^-}{\overset{K_{SS}^+}{\rightleftharpoons}} D_{SS,SS}$$

$$RS + SS \underset{K_{RS,SS}^-}{\overset{K_{RS,SS}^+}{\rightleftharpoons}} D_{RS,SS}$$

Scheme 5. Formation of diastereomer dimers. K_{RS}, K_{SS}, $K_{RS,SS}$ – the corresponding equilibrium constants. Reproduced with permission from Ref. [21] © John Wiley & Sons, Ltd., 2018.

Moreover, the back ET in excited dimers was expected to be more effective in homodimers than in heterodimers and monomers (see Scheme 6).

The CIDNP coefficients for the homodimers α are much greater than for the heterodimers of dyads β, and they are also known to differ for (*R,S*)-(*R,S*) and (*S,S*)-(*S,S*)

$$D_{RS,RS} \xrightarrow{h\upsilon} \left(RS^* : RS\right) \rightarrow \alpha_{RS} RS^{\#}$$

$$D_{SS,SS} \xrightarrow{h\upsilon} \left(SS^* : SS\right) \rightarrow \alpha_{SS} SS^{\#}$$

$$D_{RS,SS} \xrightarrow{h\upsilon} \left(RS^* : SS\right) \rightarrow \beta_{RS} RS^{\#}$$

$$D_{RS,SS} \xrightarrow{h\upsilon} \left(RS : SS^*\right) \rightarrow \beta_{SS} SS^{\#}$$

Scheme 6. UV irradiation of homo-($D_{RS,RS}$, $D_{SS,SS}$) and heterodimers ($D_{RS,SS}$) of dyads, where α and β are the CIDNP coefficients for homo- and heterodimers, and # denotes the product of back ET – polarized dyads. Reproduced with permission from Ref.[21] © John Wiley & Sons, Ltd., 2018.

homodimers ($\alpha_{RS} > \alpha_{SS}$). Note that the experimental CIDNP enhancement coefficient proved to be twice as high for (*R,S*) than for (*S,S*) diastereomers (section 2).

Here, the concentrations of dimers were assumed to be considerably higher than the concentrations of monomers. The calculation was carried out using a quasi-steady-state approximation. Because of the above assumption, the dimer stability constants have to be approximately 10^5 M^{-1} at the initial monomer concentration 10^{-3} M.

The calculated CIDNP coefficients of the diastereomers (K_c) depend on the homo- and heterodimer concentrations, stability constants of dimers and α_{RS}, α_{SS} ratio. For a detailed description of the calculation, the reader is referred to ref.[21]

The main results, demonstrating the dependence of the calculated CIDNP coefficients on the varying stability constants of the dimers, are presented in Figures 15 and 16.

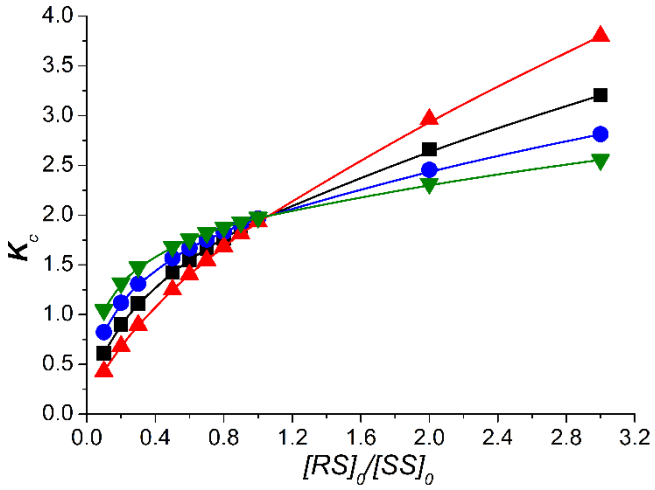

Figure 15. The results of simulating the dependence of K_c on (*R,S*) diastereomer concentration by varying the values of the homodimer stability constants. $[SS]_0 = 10^{-3}$ M, $K_{RS,SS} = 10^5$ M^{-1}, $\alpha_{SS} = 10$, $\alpha_{RS} = 20$, $\beta_{SS} = 1$, $\beta_{RS} = 1$; ■: $K_{RS} = 10^5$ M^{-1}, $K_{SS} = 10^5$ M^{-1}; ●: $K_{RS} = 2*10^5$ M^{-1}, $K_{SS} = 10^5$ M^{-1}; ▲: $K_{RS} = 5*10^4$ M^{-1}, $K_{SS} = 10^5$ M^{-1}; ▼: $K_{RS} = 2*10^5$ M^{-1}, $K_{SS} = 2*10^5$ M^{-1}. Reproduced with permission from Ref.[21] © John Wiley & Sons, Ltd., 2018.

As follows from Figure 15, K_c reaches a maximal value at the maximal difference in the values of the stability constants $K_{RS,SS}$ and K_{RS} and K_{SS}.

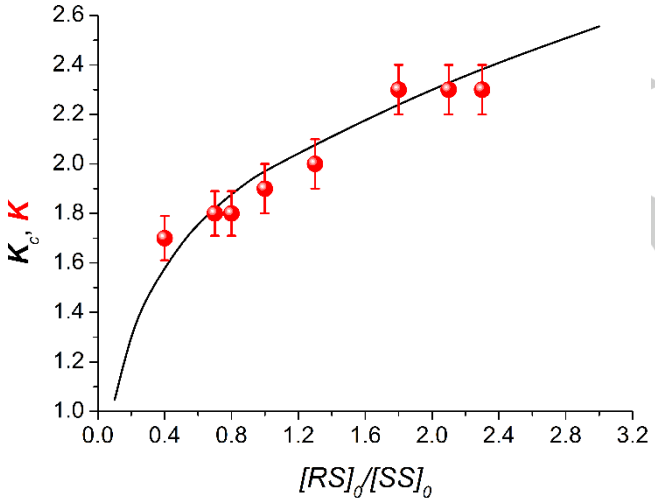

Figure 16. The experimental dependence of the observed CIDNP enhancement coefficient K (data from Table 2, red balls) and calculated K_c (black line) on (*R,S*) diastereomer concentration. $[SS]_0 = 10^{-3}$ M; $\alpha_{SS} = 10$, $\alpha_{RS} = 20$, $\beta_{RS} = 1$, $\beta_{SS} = 1$; $K_{RS} = 2*10^5$ M^{-1}, $K_{SS} = 2*10^5$ M^{-1}, $K_{RS,SS} = 1*10^5$ M^{-1}. Reproduced with permission from Ref.[21] © John Wiley & Sons, Ltd., 2018

The consistency of the modelling results and the experimental dependence of the CIDNP enhancement coefficient on the dyad concentration ratio (K_c and K), as shown in Figure 16, confirms the influence of the dimerization on the back ET.

5. Spin selectivity of ET in chiral dyads and chiral catalysis

According to the previous sections, spin selectivity, the differences between the CIDNP enhancement coefficients of the diastereomers of dyads, is explained by the differences in the HFI constants of the BZ in the (*S,S*) and (*R,S*) configurations. In addition, the results of the previous section show that a twofold difference in HFI for the (*S,S*) and (*R,S*) configurations is related to the hyperfine interaction in BZ of the (*S,S*) – (*S,S*) and (*R,S*) – (*R,S*) homodimers.

In turn, the dependence of the ratio of the CIDNP enhancement coefficients on the diastereomer concentration ratios, in accordance with Frank's theory,[3] is related to the change in the ratios of homo- and heterodimers.

If this interpretation is correct, then these results can be considered a manifestation of the catalytic influence of chiral dyad dimerization on the elementary radical process of back ET in BZs. It is reasonable to assume that in the case of ET, the mechanism of chiral catalysis is not the formation of a chiral template, as is assumed for the Soai reaction.

The influence of solvents on CIDNP enhancement coefficient ratio in dyad **2** and the dependence of the same ratio for dyad **1** on diastereomer concentration ratios can be attributed to the different impact of dimerization on the conformations of the (*R,S*) and (*S,S*) BZs.

In this regard, note that the implied mechanism of the influence of the dimerization on ET is similar to the explanation of the action of chiral monomers in the processes of enantioselective polymerization.[35,36] In that case, optically active monomers, due to their different steric effects, form polymers with different structures. The same result was found in the XRD study of dyad **2** diastereomers.[21] The (*R,S*) and (*S,S*) configurations form different H–bond: between the NH and the carboxyl oxygen and between the NH and the carbonyl group, respectively.

Therefore, to date, two possible mechanisms of chiral catalysis can be considered: catalytic action through the formation of chiral templates and through a change in the conformation of the chiral reacting particle. In the latter case, the back ET probability in the BZ of homodimer increases. In both cases, catalysts act through non-covalent weak interactions: van der Waals, donor–acceptor, dipole–dipole, and electrostatic interactions.[21,34-36]

6. Summary and outlook

This review considers the spin selectivity of ET in chiral dyads: a new peculiarity in the reactivity of chiral enantiomers as a part of diastereomers. Since spin selectivity is the result of the difference in the HFI constants of diastereomers' paramagnetic precursors, one can expect a difference in spin and electron density distributions. The latter also assumes differences in the interactions of drug enantiomers with amino acid residues located in the active sites of enzymes. Note that these

differences may be among the reasons for the sharp distinction in the medicinal activity of different enantiomers.

In addition, analysis of the spin selectivity dependence on the ratio of homo- and heterodimers of diastereomers has shown that ET in dyads **1** and **2** participates in chiral catalysis according to the Frank scheme. The assumption that the catalyst, a chiral monomer, influences the recombination probability of BZs through steric effects is consistent with the mechanism suggested for stereoselective polymerization in chiral systems.

From the abovementioned results, including the Soai reaction, the principal role of association in chiral systems is evident. However, the Soai reaction is complex process, and despite very intensive research, many questions remain open.

Therefore, the exploration of other reactions demonstrating chiral catalysis and the investigation of the impact of chiral associates on the reactions of other prochiral reagents are of great interest. Elementary reactions such as ET can prove to be useful because they enable tracing of the physical reasons for the peculiarities of chiral compound reactivity. Thus, the analysis of the dependence of the CIDNP coefficients of diastereomers on their concentration ratios indicates the impact of intermolecular interaction, specifically dimerization, on the BZ recombination probability.

The next major research focus should be examining the ability of practically important chiral compounds to form associates. These chiral associates could then become catalysts for their own synthesis. The development of new methods of absolute asymmetric synthesis of drug enantiomers is a crucial practical problem of medicinal chemistry. If the schemes described above can be applied to the alkylation of other prochiral substrates, they will provide an important breakthrough.

Acknowledgements

The work was supported by the Russian Science Foundation (18-13-00047).

Keywords: chirality • dimers • asymmetric catalysis • electron transfer • spin selectivity

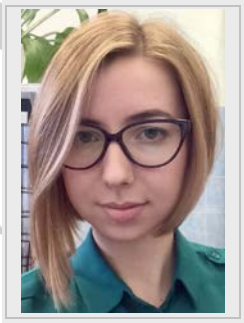

Aleksandra A. Ageeva completed her undergraduate studies in physical chemistry at Novosibirsk State University in 2016. Aleksandra is currently undertaking her PhD studies at the Voevodsky Institute of Chemical Kinetics and Combustion SB RAS on the photoinduced processes in chiral linked systems under the supervision of Prof. Tatyana Leshina.

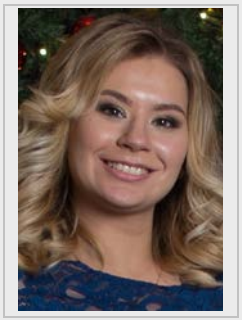

Ekaterina A. Khramtsova was born in Novosibirsk in 1992. She graduated Novosibirsk State University with a specialization in chemistry in 2013. In 2016, she received her PhD in physical chemistry from the Voevodsky Institute of Chemical Kinetics and Combustion SB RAS under the direction of Professor Tatyana Leshina. Her research interests focused on chiral drugs with special attention to the study of model systems by photochemistry and spin chemistry techniques.

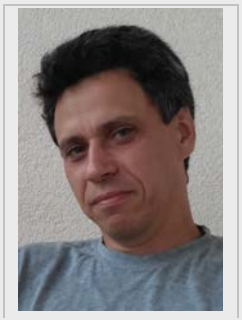

Dr. Ilya M. Magin studied Chemical Physics in Novosibirsk State University. He received a PhD from the Institute of Chemical Kinetics and Combustion Siberian Branch of the Russian Academy of Sciences, Novosibirsk in 2009 and now has a research position in the Laboratory of Magnetic Phenomena. His research interests concern theoretical descriptions and experimental investigations of electron transfer, magnetic effects, and spin dynamics in multispin and chiral systems.

Prof. Petr A. Purtov received his PhD in 1981. He earned his Dr. Sci. (Habilitation) degree in chemical physics in 2001 and the title of Professor in 2005. Currently, he is the deputy director and the head of the Laboratory of Magnetic Phenomena at the Institute of Chemical Kinetics and Combustion, Siberian Branch of the Russian Academy of Sciences, Novosibirsk. His research interests include EPR and NMR spectroscopy and their application to the study of chemical and biochemical processes, spin chemistry and its application to studying the mechanisms of radical reactions, the thermodynamics of colloid-dispersed systems, and nonequilibrium chemical thermodynamics.

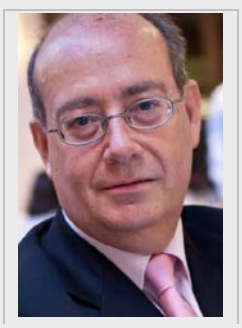

Miguel A. Miranda is a Professor of Organic Chemistry at the Polytechnical University of Valencia (Spain). The area of his research interest is on the border of photochemistry and photobiology and involves the photochemistry of biologically active organic compounds. Among his important results are the observation of stereodifferentiation in photoinduced processes with the participation of chiral NSAIDs and the study of the interactions of drugs with biomolecules. Prof. Miguel A. Miranda has been honoured with numerous awards for scientific and lecture activity.

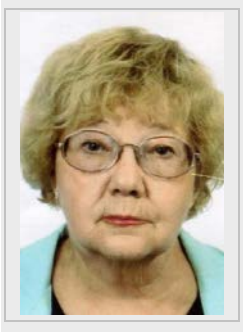

Tatyana V. Leshina has been a Professor of Physical Chemistry in the Institute of Chemical Kinetics and Combustion Siberian Branch of the Russian Academy of Sciences since 1998. She studied Chemistry and obtained her PhD degree at Novosibirsk State University. Prof. Leshina works in the area of spin chemistry. She is the author of "A new pattern of radical reactions in solution" (1998), devoted to the observation and explanation of the nature of the influence of inner and external magnetic fields on radical reactions in solutions. Today, she applies spin chemistry and photochemistry methods to study the chemical nature of the difference in medical activity of chiral drug enantiomers on model processes.

[1] M. Avalos, R. Babiano, P. Cintas, J. L. Jime´nez, J. C. Palacios, L. D. Barron, *Chem. Rev.* **1998**, *7*, 2391-2404.

[2] G.-Q. Lin, Q.-D. You, J. F. Cheng, *Chiral Drugs: Chemistry and Biological Action*, Wiley, Hoboken, **2011**, pp. 3– 29, G.-Q. Lin, Q.-D. You, J. F. Cheng, *Chiral Drugs: Chemistry and Biological Action*, Wiley, Hoboken, **2011**, pp. 323 –38.

[3] F. C. Frank, *Biochim. Biophys. Acta* **1953**, *11*, 459-463.

[4] K. Soai, T. Kawasaki, A. Matsumoto, *Acc. Chem. Res.* **2014**, *47*, 3643−3654.

[5] K. Soai, T. Kawasaki, A. Matsumoto, *Chem. Rec.* **2014**, *14*, 70–83.

[6] G. Pályi, R. Kurdi, C. Zucchi, *Advances in Asymmetric Autocatalysis and Related Topics*, Academic Press, London, **2017**, pp.1 – 22, G. Pályi, R. Kurdi, C. Zucchi, *Advances in Asymmetric Autocatalysis and Related Topics*, Academic Press, London, **2017**, pp. 183 – 195.

[7] L. Schiaffino, G. Ercolani, *Chem. Eur. J.* **2010**, *16*, 3147 – 3156.

[8] F. G. Buono, D. G. Blackmond, *J. Am. Chem. Soc.* **2003**, *125*, 8978-8979.

[9] I. D. Gridnev, A. Kh. Vorobiev, *ACS Catal.* **2012**, *2*, 2137−2149.

[10] I. D. Gridnev, J. M. Serafimov, J. M. Brown, *Angew. Chem. Int. Ed.* **2004**, *43*, 4884 –4887.

[11] M. E. Noble-Terán, J.-M. Cruz, J.-C. Micheau, T. Buhse, *Chem. Cat. Chem*. **2018**, *3*, 642–648.

[12] C. Girard, H. B. Kagan - Angew. *Chem. Int. Ed.* **1998**, *37*, 2922-2959.

[13] M. E. Noble-Teran, T. Buhse, J.-M. Cruz, C. Coudret, J.-C. Micheau, *Chem. Cat. Chem.* **2016**, *8*, 1836-1845.

[14] D. G. Blackmond, *Acc. Chem. Res.* **2000**, *33*, 402-411.

[15] A. Matsumoto, T. Abe, A. Hara, T. Tobita, T. Sasagawa, T. Kawasaki, K. Soai, *Angew. Chem. Int. Ed.* **2015**, *54*, 15218 – 15221.

[16] E.C. Ashby, I.G. Lopp, J.D. Buhler, *J. Am. Chem. Soc.* **1975**, *97*, 1964-1966.

[17] E.C. Ashby, *Acc. Chem. Res.* **1988**, *21*, 414-421.

[18] R. A. Hegstrom, D. K. Kondepudi, *Chem. Phys. Lett.* **1996**, *253*, 322-326.

[19] K. M. Salikhov, Yu. N. Molin, R. Z. Sagdeev, A. L. Buchachenko, *Spin Polarization and Magnetic Effects in Radical Reactions*, Akademiai Kiado, Budapest, Hungary, **1984**, pp. 65 – 72.

[20] C. J. Welch, K. Zawatzky, A. Makarov, S.Fujiwara, A. Matsumoto, K. Soai, *Org. Biomol. Chem.*, **2017**, *15*, 96 - 101.

[21] A. A. Ageeva, E. A. Khramtsova, I. M. Magin, D. A. Rychkov, P. A. Purtov, M. A. Miranda, T. V. Leshina, *Chem. Eur. J.* **2018**, *24*, 3882 – 3892.

[22] E. A. Khramtsova, D. V. Sosnovsky, A. A. Ageeva, E. Nuin, M. L. Marin, P. A. Purtov, S. S. Borisevich, S. L. Khursan, H. D. Roth, M. A. Miranda, V. F. Plyusnin, T. V. Leshina, *Phys. Chem. Chem. Phys.* **2016**, *18*, 12733 – 12741.

[23] E. A. Khramtsova, A. A. Ageeva, A. A. Stepanov, V. F. Plyusnin, T. V. Leshina, *Z. Phys. Chem.* **2017**, *231*, 609 – 623.

[24] I. M. Magin, N. E. Polyakov, A. I. Kruppa, P. A. Purtov, T. V. Leshina, A. S. Kiryutin, M. A. Miranda, E. Nuin, M. L. Marin, *Phys. Chem. Chem. Phys.* **2016**,*18*, 901-907.

[25] K. C. Duggan, D. J. Hermanson, J. Musee, J. J. Prusakiewicz, J. L. Scheib, B. D. Carter, S. Banerjee, J. A. Oates, L. J. Marnett, *Nature Chem. Biol.* **2011**, *7*, 803-809.

[26] K. C. Duggan, M. J. Walters, J. Musee, J. M. Harp, J. R. Kiefer, J. A. Oaters, L. J. Marnett, *J. Biol. Chem.* **2010**, *285*, 34950-34959.

[27] J. O. Miners, S. Coulter, R. H. Tukey, M. E. Veronese, D. J. Birkett, *J. Biochem. Pharmacol.* **1996**, *51*, 1003-1008.

[28] A. Levkin, H.-J. Kolb, A. I. Kokorin, V. Schurig, R. G. Kostyanovsky, *Chirality* **2006**, *18*, 232-238.

[29] V. K. Khlestkin, Yu. I. Glasachev, A. I. Kokorin, R. G. Kostyanovsky, *Mend. Commun*. **2004**, *14*, 318-320.

[30] M. Maeurer, H. B. Stegmann, *Chem. Ber.* **1990**, *123*, 1679-1685.

[31] R. W. Kreilick, J. Becher, E. F. Ullman, *J. Am. Chem. Soc.* **1969**, *91*, 5121-5124.

[32] P. Schuler, F.-M. Schaber, H. Stegman, E. Jansen, *Magn. Reson. Chem.* **1999**, *37*, 805-813.

[33] R. Naaman, D. Waldeck, *J. Phys. Chem. Lett.*, **2012**, *3*, 2178-2187.

[34] P. Yin, Z.-M. Zhang, H. Lv, T. Li, F. Haso, L. Hu, B. Zhang, J. Bacsa, Y. Wei, Y. Gao, Y. Hou, Y.-G. Li, C. L. Hill, E.-B. Wang, T. Liu, *Nat. Commun.* **2015**, *6*, 1-8.

[35] Y. Ishida, T. Aida, *J. Am. Chem. Soc.* **2002**, *124*, 14017 -14019.

[36] K. Sato, Y. Itoh, T. Aida, *Chem. Science* **2014**, *5*, 136-140.

[37] N. O. Dubinets, A. A. Safonov, A. A. Bagaturyants, *J. Phys. Chem. A* **2016**, *120*, 2779–2782.

[38] J. B. Aladekomo, J. B. Birks, *Proc. R. Soc. Lond. A* **1965**, *284*, 551-565.

[39] M. C. Jim´enez, U. Pischel, M. A. Miranda, *J. Photochem. Photobiol. C* **2007**, *8*, 128–142.

[40] M. Pracz, M. Franska, R. Franski, *J. Chem. Pharm. Res.* **2012**, *4*, 231-238.

[41] H. Kerr, R. Softley, K. Suresh, P. Hodgkinson, I. Evans, *Acta Crystallogr C Struct Chem.* **2017**, *73*, 168–175.

[42] J. Hatton, R. Richards, *Mol. Phys.* **1961**, *5*, 139–152.

[43] M. Muñoz, R. Ferrero, C. Carmona, M. Balón, *Spectrochem. Acta* **2004**, *60*, 193—200.

[44] M. Mäurer, W. Hiller, B. Müller, H. Stegmann, *Chem. Ber.* **1992**, *125*, 857-865.

10.1002/chem.201801625

WILEY-VCH

MINIREVIEW

A new example of chiral catalysis is the influence of dimerization on intramolecular electron transfer in dyads with two chiral centres. Dyad dimer formation acts in a different ways on the conformations of the paramagnetic precursors of the *(R,S)* and *(S,S)* diastereomers – biradical zwitterions. These results are in agreement with Frank's theory and its experimental confirmation - the Soai reaction.

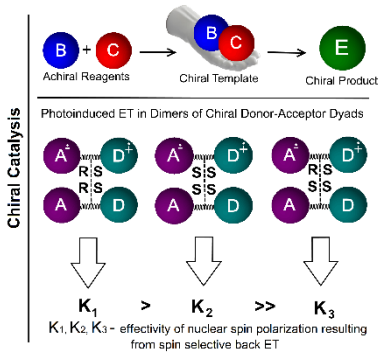

Aleksandra A. Ageeva, Ekaterina A. Khramtsova, Ilya M. Magin, Peter A. Purtov, Miguel A. Miranda, Tatyana V. Leshina*

Page No. – Page No.

Role of association in chiral catalysis: from asymmetric synthesis to spin selectivity